J Mol Model (2012) 18:3341–3350
DOI 10.1007/s00894-011-1347-2

ORIGINAL PAPER

Study of semiconducting nanomaterials under pressure

Dinesh C. Gupta · P. Rana

Received: 30 June 2011 / Accepted: 19 December 2011 / Published online: 22 January 2012

Abstract The pressure induced structural and mechanical properties of nanocrystalline ZnO, ZnS, ZnSe, GaN, CoO, CdSe, CeO_2, SnO_2, SiC, *c*-BC_2N, and β–Ga_2O_3 with different grain sizes have been analyzed under high pressures. The molecular dynamics simulation model has been used to compute isothermal equation of state, volume collapse and bulk modulus of these materials in nano and bulk phases at ambient and high pressures and compared with the experimental data. It is evident from these calculations that the change in particle size affects directly the phase transition pressure and bulk modulus. The values of phase transition pressure and bulk modulus increase with decrease in grain size of the material. The equilibrium cell volume and volume collapse in parent phase is directly proportional to the grain size of the materials. Present results are in good agreement with experimental data. The model is able to explain these thermodynamic properties at varying temperatures and pressures successfully.

Keywords Bulk modulus · Equation of state · Phase transition · Semiconductor nanomaterials · Structural properties · Volume collapse

Introduction

During last decade, the semiconducting nanomaterials have attracted attention of researchers due to unique properties *viz.*, electronic, magnetic, mechanical, optical, photonic, etc. Many of these properties are related to surface and volume effects which play an important role in characterizing their phase transformation dynamics. The transformation of a material from bulk phase to nano phase leads to change in shape of surface and surface energy along with reduction in volume which results in extra binding energy in nanomaterials as compared to their bulk counterparts. The increase in the surface energy is therefore responsible for the increase in the phase transition pressure of nanomaterials and bulk modulus, *i.e.*, reduction of compressibility in these nanomaterials. To better understand the insight mechanism of interaction mechanism, the theoretical study in particular, of the crystal properties under high pressures becomes important [1]. The survey of the literature reveals that although heaps of measured data is available on the high pressure effect on the physical properties of the semiconducting nano and bulk materials, but a very scant amount of attention has been paid theoretically on these nano materials while some theoretical results are available on a few of these bulk materials. Due to the wide range of applications, for instance, as transparent electrodes in photovoltaic and display devices, phototransistors and diodes, gas and chemical sensors, etc., the transition metal systems became quite an interesting area of research for both experimentalists and theorists [2] in the recent past due to their various technological applications [3–5].

The pressure induced structural phase transition has been observed experimentally in some semiconducting nanomaterials : ZnO (nanorods), ZnS (2.8, 5, 10 and 25.3 nm), ZnSe (nanoribbons), GaN (2–8 nm), CdSe (4.2 nm), CoO (50 nm), CeO_2 (9–15 nm), SnO_2 (3, 8, 14 nm), SiC (20, 30, 50, and 130 nm), *c*–BC_2N (5–8 nm) and β–Ga_2O_3 (14.8 ±1.9 nm), using *in-situ* energy dispersive X-ray diffraction at room temperature [6–22]. The high pressure behavior of two samples of ZnO nanorods with different grain sizes

D. C. Gupta (✉) · P. Rana
Condensed Matter Theory Group, School of Studies in Physics,
Jiwaji University,
Gwalior 474 011 MP, India
e-mail: sosfizix@yahoo.co.in

D. C. Gupta
e-mail: sosfizix@gmail.com

(sample A : diameter 150 nm, length 12000 nm and sample B : diameter 10 nm, length 230 nm) have been studied and compared with their corresponding bulk phase by Xiang et al. [6]. ZnO stabilizes in hexagonal Wurtzite structure (B4 phase) with space group (*P*63*mc*) in its ground state and transforms to rock-salt structure (B1 phase with space group $Fm\bar{3}m$) under pressure [7]. At ambient conditions, ZnS has been found in two different structures: cubic sphalerite (B3) and hexagonal (B4) and at high pressures both transform to B1 phase [8]. The structural phase transformation from B4 to B1 and B3 to B1 phases have been measured for nanocrystalline ZnS with sizes 10, 25.3, and 2.8, 5 and 10 nm [9–11]. ZnSe too crystallizes in B3 phase at ambient conditions and transforms to B1 phase at high pressures [7]. The B3 to B1 structural phase transformation has been studied in ZnSe nanoribbons with 20–80 nm thickness and width 0.2–2 μm under pressure [12]. The B4 to B1 structural phase transition from has been studied in both nano (0.2–0.8 nm) and bulk phases of wide band gap semiconductor GaN [13, 14]. It is observed by *in-situ* synchrotron radiation X-ray diffraction that CoO (50 nm) nanocrystal stabilizes in B4 phase at ambient conditions and transforms

Table 1 Values of grain size (S in nm), equilibrium cell volume V ($Å^3$), bulk modulus B_0 (GPa), pressure derivative of bulk modulus B'_0 and phase transition pressure P_T (GPa)

Materials	S	Volume		B_0	$B_0^{'}$	P_T	References
		Parent phase	Hypothetical phase				
ZnO (A) nanorod	diameter 150 length 12000	95.6	78.2	249 (WZ) 230 (RS)	4 4	8–18	Expt. [6]
ZnO (B) nanorod	diameter 10 nm length 8 nm	95.8	79.0	294 (WZ) 264 (RS)	4 4	8–27	Expt. [6]
ZnO	Bulk	95.2	78.2	164 (WZ) 206 (RS)	4 4	7 – 11	Expt. [7]
ZnS	10	38.6	-	84.9 (WZ)	4	16	Expt. [8]
		-	-	29.15 (RS)	4	-	Present
	25.3	-	-	68.5 (WZ)	7.1	15	Expt. [8]
		-	-	24.92 (RS)	4	-	Present
ZnS	Bulk	39.2	31.6	80.1 (WZ) 117.6 (RS)	4 4	12.2	Expt. [9]
ZnS	2.8	39.3	-	60.0 (ZB)	4	19	Expt. [10]
				32.19 (RS)	4	-	Present
ZnS	5	39.3	-	65.3 (ZB)	4	16.9	Expt. [11]
				29.86 (RS)	4	-	Present
ZnS	10	39.3	-	67.8 (ZB)	4	16.2	Expt. [11]
				29.99 (RS)	4	-	Present
ZnS	Bulk	38.9	31.6	38.9 (ZB) 117.6 (RS)	4 4	12.2	Expt. [9]
ZnSe nanoribbons	thickness 20-80 nm width 0.2-2 μm	33.0	-	56 (ZB) 116 (RS)	4 4	12.6	Expt. [12]
ZnSe	Bulk	45.5	37.1	69.3 (ZB) 104 (RS)	4 4	13	Expt. [7]
GaN	2-8	-	-	319 (WZ) 206 (RS)	4 4	60	Expt. [13]
GaN	Bulk	45.7	32.1	188 (WZ) 248 (RS)	3.2 5.5	37	Expt. [14]
CoO	50	-	-	115 (WZ) 270 (RS)	2.8 3.4	6.9	Expt. [15]
CdSe	4.2	56.2	43.6	37 (WZ) 74 (RS)	11 4	3	Expt. [16]
CeO_2	9-15	159.2	130.5	328 ($Fm\bar{3}m$) 326 (Pnma)	4 4	22.3	Expt. [17]
CeO_2	Bulk	158.4	122.0	230 ($Fm\bar{3}m$) 304 (Pnma)	4 4	31.5	Expt. [18]

Table 2 Values of grain size (S in nm), lattice constants (Å), bulk modulus B_0 (GPa), and pressure derivative of bulk modulus B'_0 in ground phase of nanomaterials

Materials	S	Lattice constant	B_0	B'_0	References
SnO_2	3	a=4.72	257	2.3	Expt. [19]
	8	c=3.18	228	5.6	
	14	-	225	6	
	Bulk	-	277	4	
SiC	20	-	260±39	4	Expt. [20]
	30	-	241±17	4	
	50	-	198±12	4	
	130	-	193±6	4	
c-BC_2N	5-8	a=3.59	420±11[a]	3.4	Expt. [21]
c-BC_2N	5-8	a=3.59	350±17[b] Ψ=90°	4	Expt. [21]
c-BC_2N	5-8	a=3.59	276±20[b] Ψ=54.7°	4	Expt. [21]
c-BC_2N	5-8	a=3.59	184±17[b] Ψ=0°	4	Expt. [21]
β-Ga_2O_3	14.8±1.9	a=12.2 b=3.04 c=5.8 β=103.7±0.3	191±4.9	8.3±0.9	Expt. [22]

[a] axial X-ray diffraction data [b] radial X-ray diffraction data

to B1 phase under pressure [15]. The effect of size on stability of CdSe nanocrystal (4.2 nm) under high pressures has been investigated by X-ray diffraction and optical absorption techniques [16]. CeO_2 stabilizes in cubic fluorite structure ($Fm\bar{3}m$) and shows transformation to orthorhombic (Pnma) structure in both nano and bulk phases [17, 18]. The very useful and demandable semiconducting SnO_2 with different particle sizes transforms from rutile to cubic $CaCl_2$ structure under pressure [19]. The variation of bulk modulus (B_0) of nano SiC has been studied and compared with its corresponding bulk phase under the influence of high pressures for four different sets of nanoparticles [20]. *c*–BC_2N has attracted interest of researchers due to its super hardness. The stress behavior of nanocrystalline *c*–BC_2N has been analyzed by using the axial and radial X-ray diffraction under non-hydrostatic pressures at different radial angles (ψ=0°, 57.4° and 90° represented by circle, square and triangle, respectively) [21]. Transmission electron microscopy and X–ray diffraction techniques have been used to estimate the mean size of the optically transparent material β–Ga_2O_3 with monoclinic structure (a=12.2, b=3.04, c=5.8, β = 103.7±0.3) which shows the material transforms to α–Ga_2O_3 structure under pressure [22].

These materials exhibit structural phase transition to various phases under pressure. Sufficient experimental data is available on high pressure and temperature studies of these nanocrystalline materials but they are much less explored theoretically. Hence, the high pressure study of these nano materials still requires more theoretical attention to analyze them properly.

We have used a thermodynamic method to analyze the structural and mechanical properties of these nanomaterials with different grain sizes along with their bulk phases under compression. In the present study, we have devoted efforts to give a comprehensive theoretical study on the high pressure behavior of some semiconductor and dielectric nanomaterials with different particle sizes along with their bulk forms at constant temperature.

Methodology

The molecular dynamics (MD) simulation method has been used to analyze the thermodynamic properties of nanomaterials. It simulates the motion of atoms and molecules interacting with specific interatomic potentials [23] and allows studying the dynamics of the system at finite temperatures as these properties are related to interatomic distances between atoms. Many characteristics of nanomaterials are related to their surface and volume effects and any change in

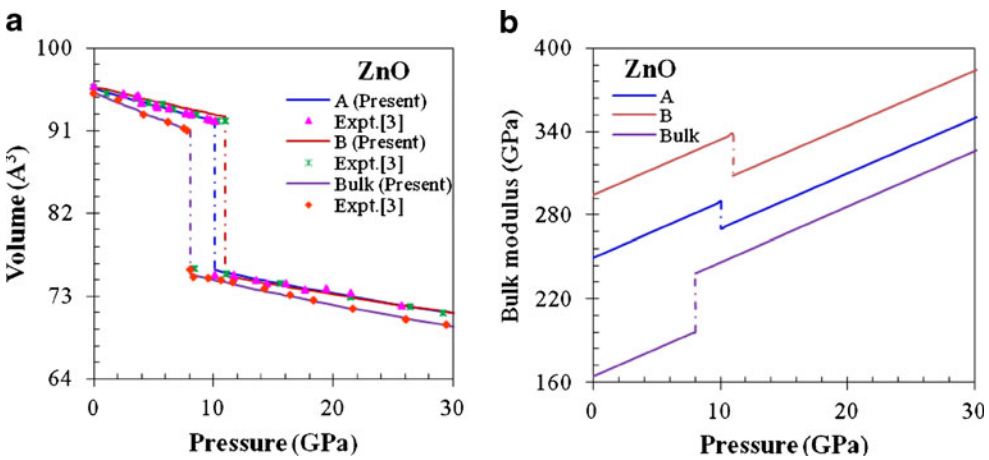

Fig. 1 (**a**) The variation of relative volume with pressure for nano (A, B) and bulk ZnO. (**b**) The pressure dependence of bulk modulus for nano (A, B) and bulk ZnO

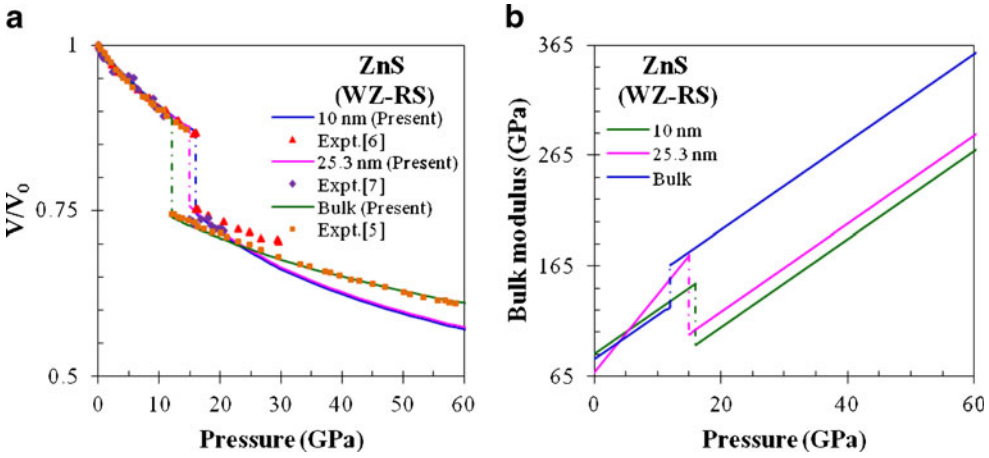

Fig. 2 (**a**) The phase diagram of ZnS in nano (10 and 25.3 nm) and bulk phases in B4 and B1 phases. (**b**) Pressure dependence of bulk modulus for nano (10 and 25.3 nm) and bulk ZnS

their dimensions are directly related to the change in their corresponding temperature and / or pressure. As the temperature and / or pressure of material vary, it affects the density of material which indicates the thermal expansion within the material. The well-known expression for volume thermal expansion coefficient (α) with the cell volume (V) at a particular temperature (T) is given as:

$$\alpha = \frac{1}{V}\left(\frac{\partial V}{\partial T}\right)_P, \tag{1}$$

which gives αB_T=constant.

The solution of the above equation at constant pressure can be obtained as

$$\alpha\left(\frac{\partial B_T}{\partial T}\right)_P + B_T\left(\frac{\partial \alpha}{\partial T}\right)_P = 0. \tag{2}$$

At initial boundary conditions, *i.e.,* $T=T_0$ and $\alpha=\alpha_o$, the above expression gives:

$$\frac{V}{V_0} = [1 - \alpha_o \delta_T (T - T_0)], \tag{3}$$

where δ_T is thermo-elastic Anderson-Gruneisen parameter

$$\delta_T = -\frac{1}{\alpha B_T}\left(\frac{\partial B_T}{\partial T}\right). \tag{4}$$

The thermal pressure (P_{th}) can be defined as [24]

$$P_{th} = \alpha_o B_0 (T - T_0), \tag{5}$$

where B_0 is isothermal bulk modulus at temperature T_0. One can re-write Eq. 3 as:

$$\frac{V}{V_0} = \left[1 - \frac{\delta_T}{B_0} P_{th}\right]^{\frac{-1}{\delta_T}}. \tag{6}$$

When the system is studied under high pressures the above expression appears to be:

$$P_{th} = \frac{B_0}{\delta_T}\left[1 - \left(\frac{V}{V_0}\right)^{-\delta_T}\right] + P. \tag{7}$$

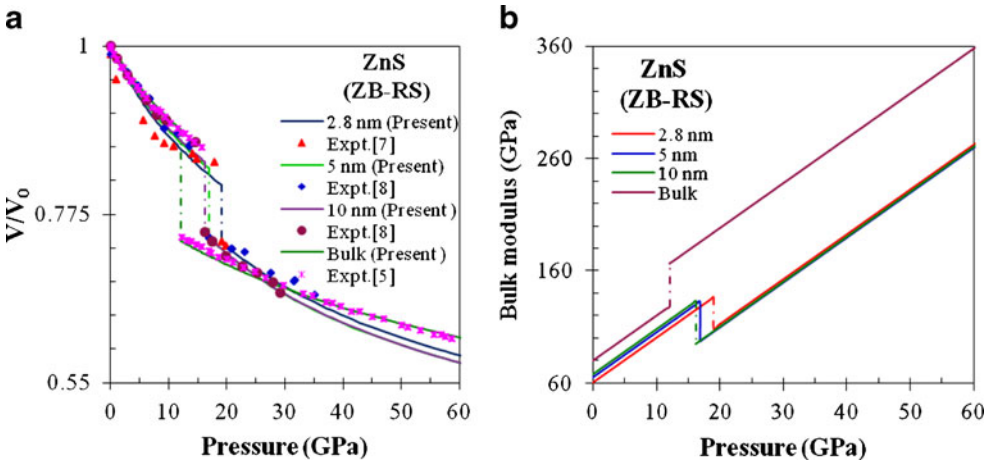

Fig. 3 (**a**) Pressure dependence of relative volume of ZnS in nano (2.8, 5 and 10 nm) and bulk phases for B3 to B1 transition. (**b**) Pressure dependence of bulk modulus of ZnS in nano (2.8, 5 and 10 nm) and bulk phases for B3 to B1 transition

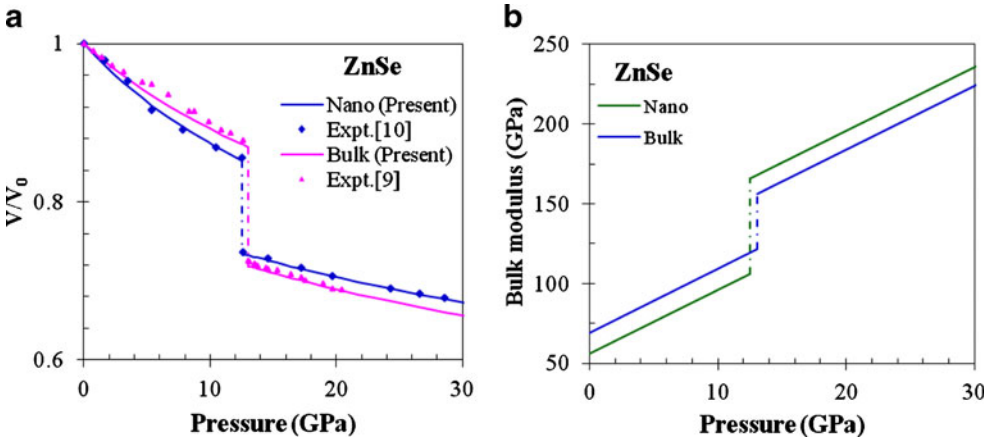

Fig. 4 (**a**) Pressure dependence of relative cell volume of ZnSe nano and bulk phases. (**b**). Pressure dependence of bulk modulus in ZnSe nano and bulk phases

At ambient conditions $P_{th}=0$, which reduces the above equation to

$$P = -\frac{B}{B'_0}\left[1-\left(\frac{V}{V_0}\right)^{-\delta_T}\right] \tag{8}$$

By using the approximation, $\delta_T=B'_0$ [18], the first-order derivative of isothermal bulk modulus

$$P = -\frac{B}{B'_0}\left[1-\left(\frac{V}{V_0}\right)^{-B'_0}\right] \; or \; \frac{V}{V_0}=\left[1+\left(\frac{B'_0}{B}\right)P\right]^{\frac{-1}{B'_0}}. \tag{9}$$

The above expression is a widely used basic expression required for the present formulation, *i.e.,* Murnaghan's equation of state (EOS). The above formulation is based on equilibrium conditions, *i.e.*, $V=V_0$, hence

$$B = B_0 + B'_0(P - P_0) \tag{10}$$

shows the dependence of bulk modulus (B) with pressure. Here, all the parameters have their usual meanings

$B_0=-V(\partial P/\partial V)_T$, the equilibrium isothermal bulk modulus,

$B'_0=(\partial B/\partial P)_T$, the first-order pressure derivative of B, with

P and $P_0=-\partial E/\partial V$, the pressure which is defined as the negative derivative of the total energy.

Results and discussion

The structural phase transition and mechanical properties of a variety of nanomaterials and their bulk phases have been analyzed by using MD simulation method as discussed above. For this purpose, the reduced volumes (V/V_0) have been calculated at different pressures from above formulation to obtain the isothermal equation of state (EOS) of the present set of bulk and nanomaterials. From the EOS of both nano and corresponding bulk structures, it is observed that nano phase of these materials can have more useful applications than their bulk counterparts. The values of input data and some basic information about the present set of nanomaterials and bulk counterparts have been reported in Tables 1 and 2.

ZnO

The phase diagram of two different nano samples (A and B) and bulk phase of ZnO has been plotted along with

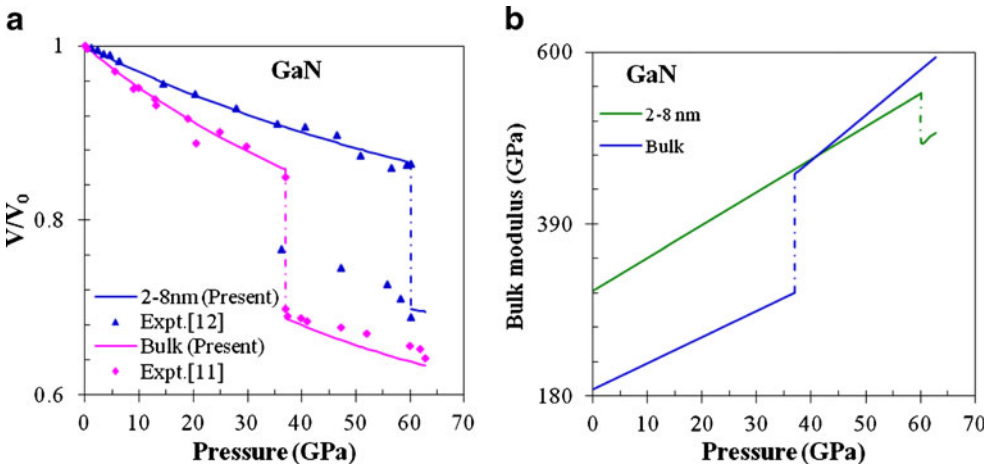

Fig. 5 (**a**) Pressure dependence of relative cell volume of GaN in nano and bulk phases. (**b**) Pressure dependence of bulk modulus of GaN nano and bulk phases

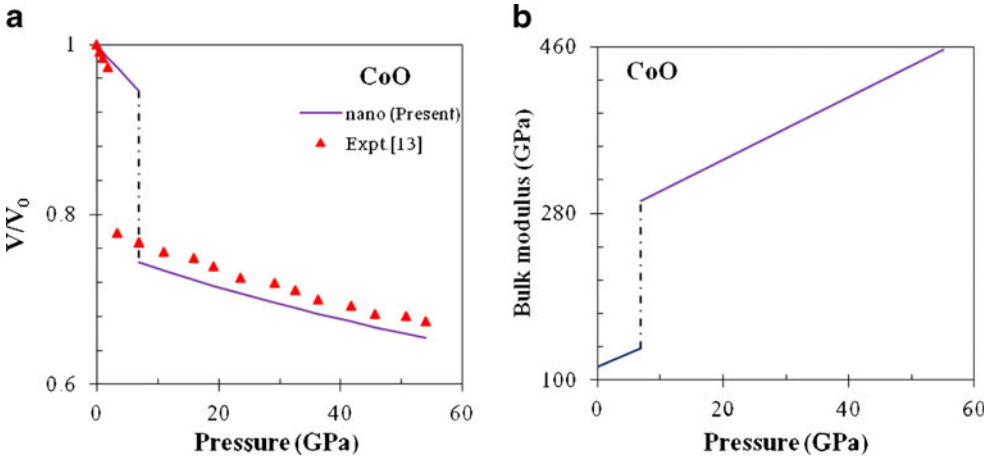

Fig. 6 (**a**) Pressure dependence of relative cell volume of CoO nano particles. (**b**) Pressure dependence of bulk modulus in CoO nano particles

experimental data in Fig. 1a. It may be found from this figure that ZnO is stable in B4 phase at ambient conditions and under pressure it transforms to a more compressed B1 phase at transition pressure (P_T=~10 GPa) in both the nano samples (A and B) while the bulk phase of ZnO shows transformation at ~9 GPa [6, 7]. The calculated values of structural transformation are associated with the relative volume collapse ($\Delta V(P_T)/V(0)$) of 17.7, 17.4 and 17.27% in nanorods (A and B) and bulk structures which are quite close to the experimental values 17.8, 17.6 and 17.3% [6]. The pressure dependence of bulk modulus has also been plotted for all three samples of ZnO in Fig. 1b. It has been observed that the bulk modulus increases linearly in both B4 as well as B1 phases in nanorod samples A and B of ZnO and shows an abrupt decrease at P_T. In bulk ZnO, although, it has similar linear variation in both the phases but it shows an abrupt increase at P_T which is just opposite to what is found in the nano samples of this material. It is further observed that as the particle size increases the compressibility of the material decreases and approaches the values of its bulk phase.

ZnS

At ambient conditions, ZnS stabilizes in two crystal structures: Wurtzite (B4) and zincblende (B3) followed by phase transformation to rock-salt (B1 phase) structure at high pressures in both nanocrystalline and bulk phases [8–11].

The pressure induced structural phase transformations from B4 to B1 phase has been studied for 10 and 25.3 nm samples of nanocrystalline ZnS. The pressure dependence of relative volume (V/V_0) and bulk modulus for these samples of ZnS have been plotted along with their bulk phase in Figs. 2a–b and compared with experimental data. Figure 2a shows that the nanocrystalline ZnS with B4 phase remains stable up to 16 GPa for 10 nm and 15 GPa for 25.3 nm and beyond these pressures they transform to B1 phase, whereas its bulk counterpart shows the phase transformation at comparatively low pressure, *i.e.*, at 12.2 GPa. This phase transformation (B4→B1) is accompanied by relative volume collapse of 12.39% for 10 nm, 11.99% for 25.3 nm samples and 14.92% for its bulk phase. These values are close to the experimental [8–10] data 12.96%, 11.69% and 14.80%. From Fig. 2b, it may be seen that bulk modulus increases linearly with pressure followed by an abrupt decrease at P_T in nano ZnS while the trend is reversed in its bulk phase.

The EOS for B3→B1 transformation in nano ZnS with particle sizes 2.8, 5 and 10 nm and in its bulk phase has been depicted in Fig. 3a along with their experimental values. The phase transition occurs at 19, 16.9 and 16.2 GPa in 2.8, 5 and

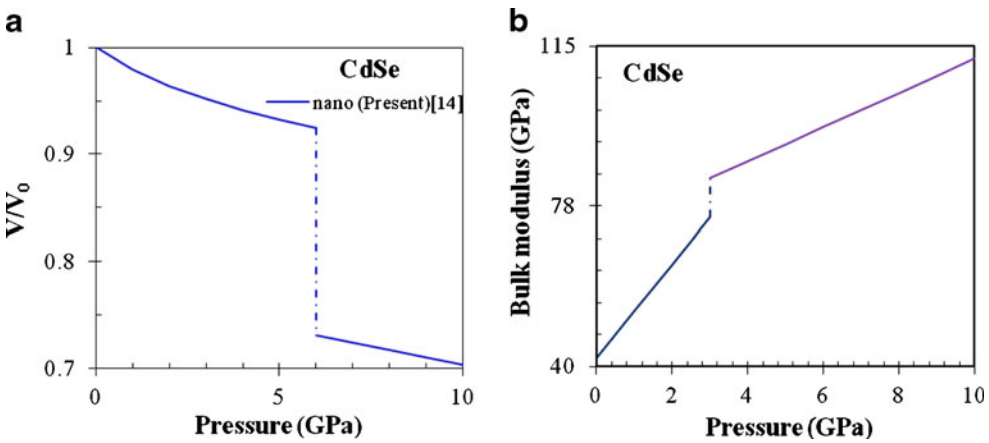

Fig. 7 (**a**) Pressure dependence of volume change in relative cell of CdSe nanoparticles. (**b**) Pressure dependence of bulk modulus in CdSe nanoparticles

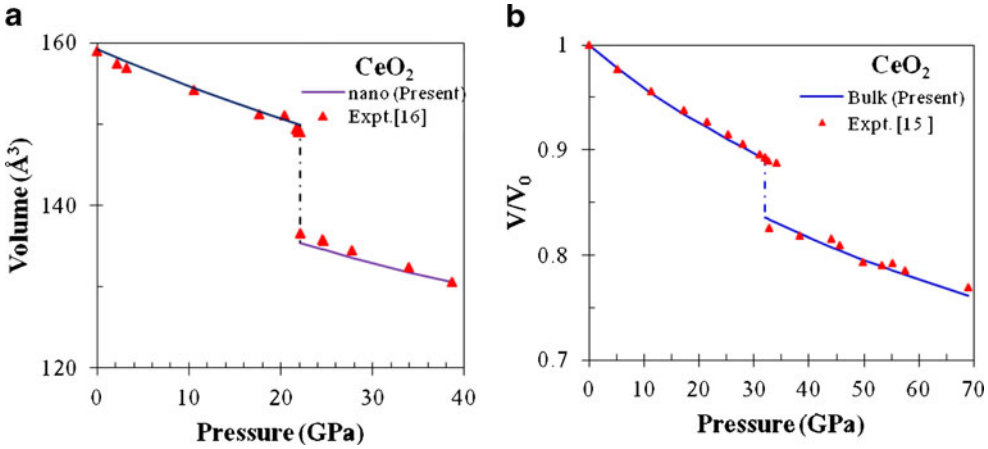

Fig. 8 (**a**) Pressure dependence of volume change in unit cell of CeO_2 nanoparticles. (**b**) Pressure dependence of bulk modulus of CeO_2 nanoparticles

10 nm ZnS, respectively. From this figure it is observed that P_T increases as the particle size decreases while the volume collapse decreases with decrease in particle size. The relative volume collapse at P_T has been calculated to be 7.64% for 2.8 nm, 9.32% for 5 nm and 9.56% for 10 nm and 14.83% in bulk ZnS. These results agree well with the experiments data [8–11]. The pressure dependence of bulk modulus for these nano and bulk crystals of ZnS is shown in Fig. 3b. The trend of variation is similar as seen in nano ZnO.

ZnSe

The nano as well as bulk ZnSe crystallize in B3 phase at ambient conditions. Under pressure, it transforms to B1 phase. The pressure dependence of calculated relative cell volume for nanocrystalline and bulk ZnSe has been plotted in Fig. 4a while the variation of bulk modulus with pressure in Fig. 4b along with their experimental values. Figure 4a shows that P_T of ZnSe nanoribbons of thickness 20–80 nm and width 0.2-2 μm and bulk ZnSe remains close to each other. The computed value of volume collapse, 12.76% at P_T=12.6 GPa for nanoribbons and 15.04% at P_T=13 GPa for bulk ZnSe, are close to their measured value of 13% for nanoribbons and 15% for bulk phase [7, 12]. The variation of bulk modulus with the pressure behaves differently as compared to that in other members of this family, *i.e.*, ZnO and ZnS. The bulk modulus in both nanoribbons and bulk phase shows similar nature of variation, *i.e.*, it increases linearly and shows an abrupt increase at P_T.

GaN

The EOS has been computed for both nano and bulk phases of GaN. These values have been plotted in Fig. 5a along with their experimental data. The P_T is 60 GPa for nano GaN [14] while the transformation occurs at much lower pressure, *i.e.*, at 37 GPa in bulk GaN [13]. The relative volume collapse has been calculated to be 17.1% and 17.52% for both nano and bulk GaN which agree well with the measured data 16.9% and 17% [13, 14]. The variation of bulk modulus *vs*. pressure for nano and bulk GaN has been shown in Fig. 5b. It is observed from this figure that in nanocrystalline GaN, the bulk modulus increases linearly with pressure followed by an abrupt decrease at P_T which signifies that the compressibility of the material decreases as pressure increases, while its nature of variation is found to be just opposite in bulk GaN.

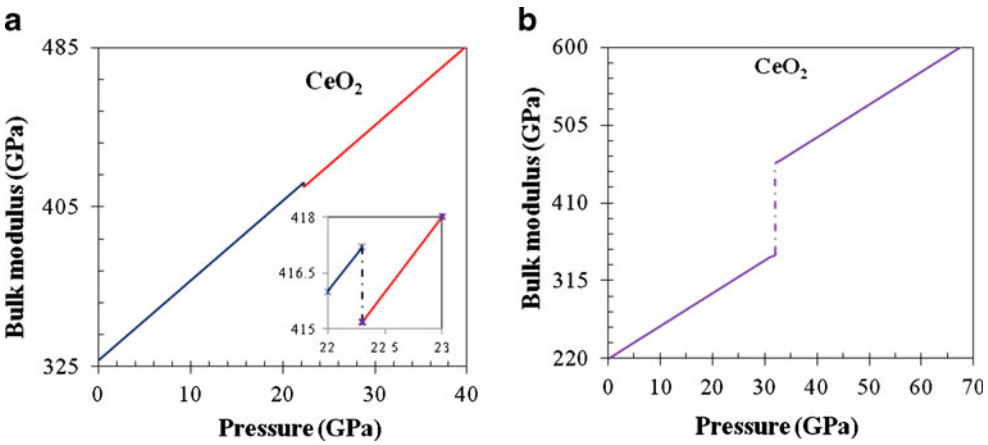

Fig. 9 (**a**) Pressure dependence of change in volume of CeO_2 in bulk phase. (**b**) Pressure dependence of bulk modulus of CeO_2

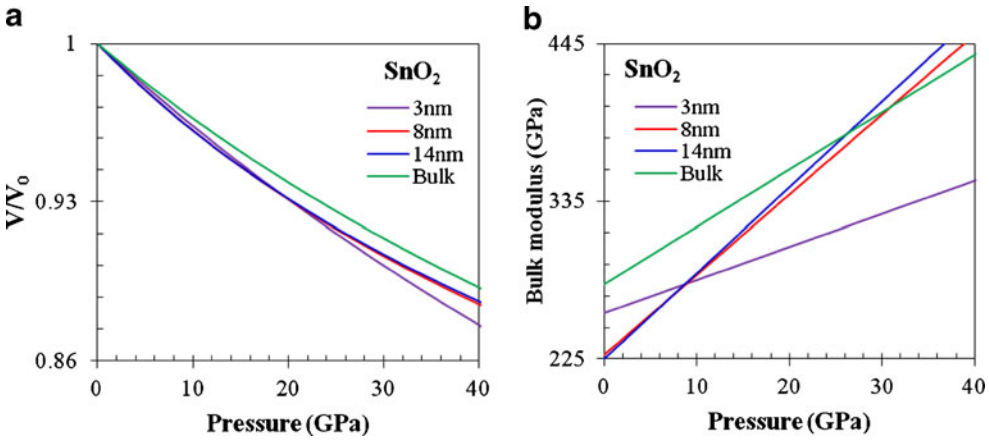

Fig. 10 (**a**) Pressure dependence of change in volume of SnO_2 (3, 8, 14 nm) and in bulk phases. (**b**) Pressure dependence of bulk modulus of SnO_2 (3, 8, 14 nm) and in bulk phases

CoO

The nanocrystalline CoO with 50 nm size shows structural phase transformation from B4→B1 phase under pressure. The EOS for nano phase of CoO has been plotted in Fig. 6a. The estimated relative volume collapse for B4 → B1 transition is 20.15% (at P_T=6.93 GPa) which is quite close to the experimental value of 20% [15]. The pressure dependence of bulk modulus in ground and high pressure phases has been depicted in Fig. 6b. It may be concluded from this figure that the nature of variation of bulk modulus is different than that found in other nanomaterials under consideration. This variation resembles with the trend found in bulk phase of other materials chosen in the present study.

CdSe

The computed EOS has been depicted in Fig. 7a for nano CdSe (4.2 nm) in B4 and B1 phases, shows 19.33% volume collapse at P_T=6 GPa which is close to its measured value of 20% [16]. The variation of bulk modulus with pressure in both B4 and B1 phases has been plotted in Fig. 7b. It may be observed that the bulk modulus in both the phases increases with the increase in pressure with an abrupt increase at P_T. This behavior is different from that has been observed in the present set of nanomaterials and resembles the nature as found in nanocrystalline CoO (as discussed above) and bulk materials.

CeO_2

The study of high pressure behavior of CeO_2 reveals that the material shows structural phase transition from cubic fluorite to orthorhombic (α–$PbCl_2$) structure in its nano and bulk phases. Nanocrystalline CeO_2 with particle size 9–15 nm undergoes phase transition at 22.3 GPa which is smaller than the value (P_T=31.5 GPa) found for bulk CeO_2 [17, 18]. The EOS of nano CeO_2 along with their experimental values have been plotted in Fig. 8a. This structural phase transition is associated with 9.75% reduction in cell volume which is complementary to its experimental value 9.4%. The pressure dependence of relative volume for bulk CeO_2 has been depicted in Fig. 8b. This figure shows the structural phase transformation from cubic fluorite to orthorhombic α-$PbCl_2$ structure with volume collapse of 7.7% which is close to its measured value of 7.5±0.7%. The variation of bulk modulus *vs.* pressure for nanocrystalline CeO_2, is shown in Fig. 9a, which concludes that the material follows a similar trend as

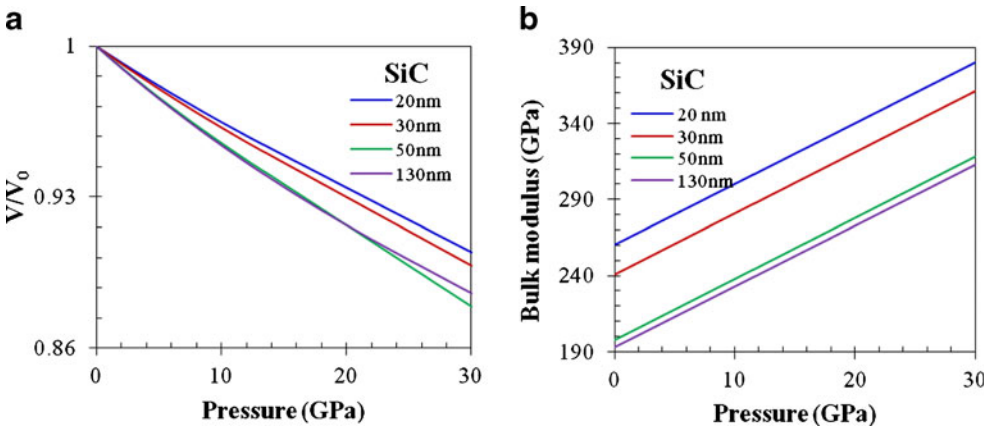

Fig. 11 (**a**) Pressure dependence of change in volume of SiC (20, 30, 50 and 130 nm). (**b**) Pressure dependence of bulk modulus of SiC

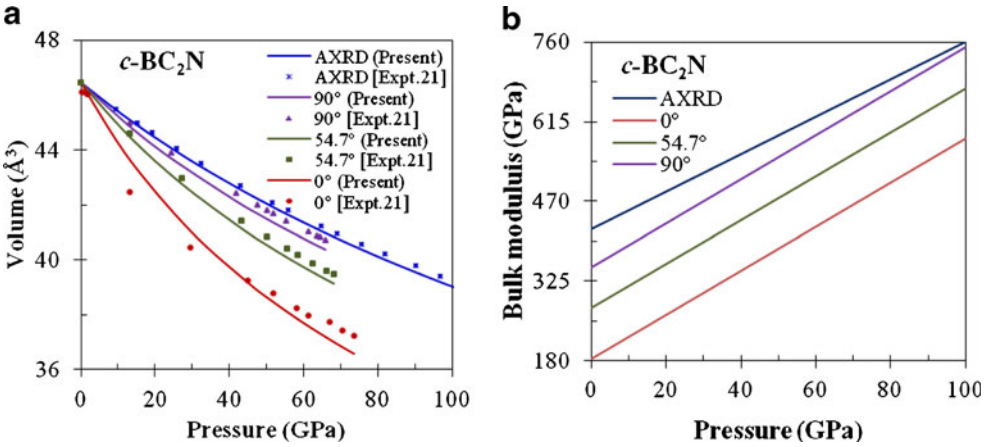

Fig. 12 (**a**) Pressure dependence of change in volume of c-BC_2N 5–8 nm, 5–8 nm for Ψ=0°, 5-8 nm for Ψ=57.4°, 5-8 nm for Ψ=90°). (**b**) Pressure dependence of bulk modulus of c-BC_2N

found in other nanocrystalline compounds. The inset in this figure clearly highlights the effect of particle size on the compressibility of the material. The pressure dependence of bulk modulus in bulk CeO_2 is reported in Fig. 9b. The variation of B_T with pressure shows abrupt increase in bulk CeO_2 while it shows an abrupt decrease in its nano phase at P_T. On comparing the nature of bulk modulus with pressure in both phases, it is clear that the compressibility of the material decreases with reduction in size of material.

SnO_2

The calculated values of reduced volume *vs*. pressure has been plotted in Figs. 10a-b to obtain the EOS of nanocrystalline SnO_2 with three different particle sizes 3, 8, and 14 nm and their bulk phase. This figure shows the linear decrease of V/V_0 with pressure. In bulk phase, its value decreases slowly while reducing the size of the particle, the relative volume decreases rapidly with pressure and has minimum value for sample with 3 nm particles. The variation of B_T with pressure has been shown in Fig. 10b which shows that B_T increases with pressure. Also its value increases with the decrease in particle size, *i.e.*, the compressibility of the material decreases with size in nanoparticles. The bulk modulus is found to be much higher than nanoparticles [19] as reported in Table 2.

SiC

The pressure dependence of relative cell volume has been depicted in Fig. 11a for nanocrystalline SiC. This figure shows the same trend of variation for all sizes of SiC. As the grain size varies from 20 nm to 130 nm the material becomes more compressible. The nature observed here is completely opposite to nano phase of SnO_2. The pressure dependence of bulk modulus for nanocrystalline SiC with different sizes (20, 30, 50 and 130 nm) has been reported in Fig. 11b, which shows that the bulk modulus increases linearly with pressure. It proves that the compressibility of the material decreases with increase in particle size.

c-BC_2N

Nanocrystalline *c*-BC_2N with sizes 5–8 nm have been studied under high pressures using axial X-ray diffraction (AXRD) method [21] at three different radial angles (ψ= 0°, 57.4° and 90° represented by circle, square and triangle, respectively). We have calculated EOS for all three samples

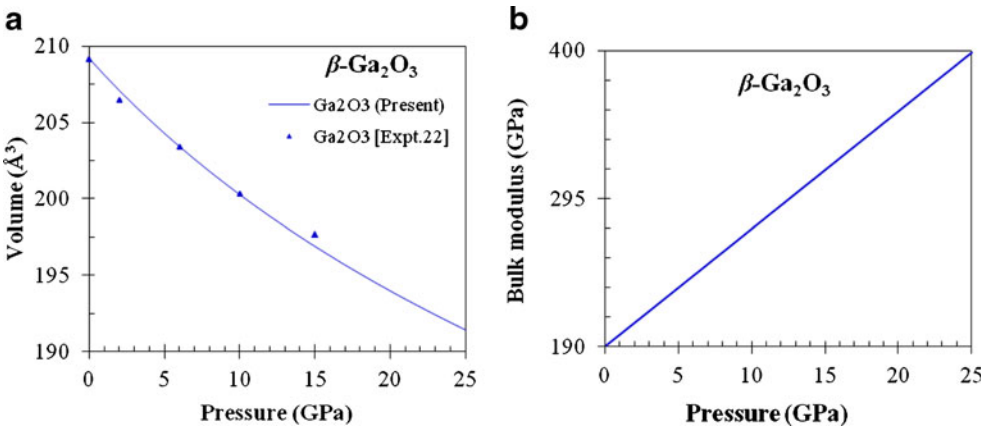

Fig. 13 (a) Pressure dependence of change in volume of β-Ga_2O_3 (14.8 ± 1.9 nm). (b) Pressure dependence of bulk modulus of β-Ga_2O_3

and presented them along with their experimental data in Fig. 12a. It is seen from this figure that the variation of relative cell volume ratio decreases slowly as we change the radial angle from 0° to 90°, while it remains lowest in the case of sample under axial study. The order of variation is found to be reversed for bulk modulus as can be seen from Fig. 12b. The bulk modulus is maximum for sample studied under AXRD while minimum for sample studied at $\psi=0°$. It is also found that bulk modulus increases linearly with increase in pressure in all four samples.

β-Ga_2O_3

The pressure dependence of relative volume and bulk modulus as function of pressure has been computed for optically transparent β-Ga_2O_3 nanocrystals having particle size 14.8± 1.9 nm. The EOS has been depicted in Figs. 13a along with experimental data [22]. This figure shows that the relative volume for nano β-Ga_2O_3 decreases linearly with the increase in pressure. The variation of bulk modulus as a function of pressure has been plotted in Figs. 13b which shows the linear increase of bulk modulus with pressure.

Conclusions

We have performed simulation study of the structural properties of some semiconducting nanocrystalline materials and their bulk forms at ambient and high pressures. The physical properties of the nanomaterials depend on the surface energy and volume effects which are responsible for the size of the particle size of material. It is found that the particle size of the material significantly affects its structural properties, *viz.*, P_T, equilibrium cell volume, bulk modulus, etc. In the present set of nanomaterials, it is observed that

the transition pressure (P_T) of nanomaterials increases appreciably as compared to their bulk form, *i.e.,* the decrease in grain size increases P_T, excluding CeO_2 where P_T decreases with decrease in material grain size.

The bulk modulus in the nano phase of the materials is comparatively higher than that of bulk counterpart in their ground state which leads to the conclusion that the nanomaterials have less compressibility.

Generally, % volume collapse reduces with the decrease in particle size in most of the nanomaterials analyzed in this article expect ZnO and GaN.

The results obtained by us are close to their experimental data. Since, there is lack of other theoretical studies on the high pressure behavior of these nanoparticles, hence future results may certainly testify these results.

Acknowledgments The work is financially supported by Department of Science and Technology (DST), New Delhi, India.

References

1. Ganguli AK, Ahmad T, Vaidya S, Ahmed J (2008) Pure Appl Chem 80:2451–2477
2. Jaffe JE, Snyder JA, Lin Z, Hess AC (2000) Phys Rev B 62:1660–1665
3. Tarascon JM, Armand M (2001) Nature 414:359–367
4. Zeng H, Li J, Liu JP, Wang ZL, Sun S (2002) Nature 420:395–412
5. Skumryev V, Stoyanov S, Zhang Y, Hadjipanayis G, Givord D, Nogues J (2003) Nature 423:850–853
6. Wu X, Wu Z, Guo L, Liu C, Liu J, Li X, Xu H (2005) Solid State Commun 135:780–784
7. Karzel H, Potzel W, Kofferlein M, Schiessl W, Steiner M, Hiller U, Kalvius GM (1996) Phys Rev B 53:11425–11438
8. Yue-Wu P, Sheng-Chun Q, Chun-Xiao G, Yong-Hao H, Ji-Feng L, Qi-Liang C, Jing L, Guang-Tian Z (2004) Chin Phys Lett 21:67–69
9. Desgreniers S, Beaulieu L, Lepage I (2000) Phys Rev B 61:8726–8733
10. Qadri SB, Skelton EF (2001) J Appl Phys 89:115–119
11. Pan Y, Yu J, Hu Z, Li H, Cui Q, Zou G (2007) J Mater Sci Technol 23:193–195
12. Yao LD, Wang FF, Shen X, You SJ, Yang LX, Jiang S, Li YC, Zhu K, Liu YL, Pan AL, Zou BS, Liu J, Jin CQ, Yu RC (2009) J Alloys Compds 480:798–801
13. Jorgensen JE, Jakobsen JM, Jiang JZ, Gerward L, Olsen JS (2003) J Appl Cryst 36:920–925
14. Xia H, Xia Q, Ruoff AL (1993) Phys Rev B 47:12925–12928
15. Liu JF, He Y, Chen W, Zhang GQ, Zeng YW, Kikegawa T, Jiang JZ (2007) J Phys Chem C 111:2–5
16. Tolbert SH, Alivisatos AP (1995) J Chem Phys 102:4642–4656
17. Wang Z, Saxena SK, Pischedda V, Liermann HP, Zha CS (2001) Phys Rev B 64:012102
18. Duclos SJ, Vohra YK, Ruoff AL (1988) Phys Rev B 38:7755–7758
19. He Y, Liu JF, Chen W, Wang Y, Wang H, Zeng YW, Zhang GQ, Wang LN, Liu J, Hu TD, Hahn H, Gleiter H, Jiang JZ (2005) Phys Rev B 72:212102
20. Rich RM, Stelmakh S, Patyk J, Wieligor M, Zerda TW, Guo Q (2009) J Mater Sci 44:3010–3013
21. Dong H, He D, Duffy TS, Zhao Y (2009) Phys Rev B 79:014105
22. Lipinska-Kalita KE, Chen B, Kruger MB, Ohki Y, Murowchick J, Gogol EP (2003) Phys Rev B 68:035209
23. Prakash N (2005) Master of Science Thesis. The Florida State University, Tallahassee
24. Anderson OL (1995) Equation of State of Solids for Geophysics and Ceramic Science. Oxford University Press, Oxford